



1 October 7, 2020

2

3 **Temperature decadal trends, and their relation to diurnal variations in the lower**  
4 **thermosphere, stratosphere, and mesosphere, based on measurements from SABER on**  
5 **TIMED.**

6

7 **Frank T. Huang<sup>1\*</sup>, Hans G. Mayr<sup>2\*</sup>**

8 <sup>1</sup>University of Maryland, Baltimore County, MD 21250, USA

9 <sup>2</sup>NASA Goddard Space Flight Center, Greenbelt, MD 20771, USA

10 \*retired

11

12 **Abstract.** We have derived the behavior of decadal temperature trends over the 24 hours of local  
13 time, based on zonal averages of SABER data, years 2012 to 2014, 20 to 100 km, within 48° of  
14 the equator. Similar results have not been available previously. We find that the temperature  
15 trends, based on zonal mean measurements at a fixed local time, can be different from those  
16 based on measurements made at a different fixed local time. The trends can vary significantly in  
17 local time, even from hour to hour. This agrees with some findings based on night-time lidar  
18 measurements. This knowledge is relevant because the large majority of temperature  
19 measurements, especially in the stratosphere, are made by instruments on sun-synchronous  
20 operational satellites which measure at only one or two fixed local times, for the duration of their  
21 missions. In these cases, the zonal mean trends derived from various satellite data are tied to the  
22 specific local times at which each instrument samples the data, and the trends are then also  
23 biased by the local time. Consequently, care is needed in comparing trends based on various  
24 measurements with each other, unless the data are all measured at the same local time. A similar  
25 caution is needed when comparing with models, since the zonal means from 3D models reflect  
26 averages over both longitude and the 24 hours of local time. Consideration is also needed in  
27 merging data from various sources to produce generic, continuous longer-term records. Diurnal  
28 variations of temperature themselves, in the form of thermal tides, are well known, and are due  
29 to absorption of solar radiation. We find that at least part of the reason that temperature trends  
30 are different for different local times is that the amplitudes and phases of the tides themselves  
31 follow trends over the same time span of the data. Much of past efforts have focused on the  
32 temperature values with local time when merging data from various sources, and on the effect of  
33 unintended satellite orbital drifts, which result in drifting local times at which the temperatures  
34 are measured. However, the effect of local time on trends has not been well researched. We also  
35 derive estimates of trends by simulating the drift of local time due to drifting orbits. Our  
36 comparisons with results found by others (AMSU, lidar) are favorable and informative. They  
37 may explain at least in part, the bridge between results based on daytime AMSU data and night  
38 time lidar measurements. However, these examples do not a pattern make, and more  
39 comparisons and study are needed.

40

41 **1 Introduction**

42 The understanding of decadal temperature trends in the middle and upper atmosphere is  
43 interesting scientifically and important for practical reasons. Global temperature trends have  
44 been researched for decades based on a variety of satellite and ground-based measurements.  
45 However, relatively few studies have focused on the behavior of trends as a function of local  
46 time. Past efforts have focused more on the local time variations of temperature themselves in



47 comparing or merging various data sets, and on accounting for drifts in local time of  
48 measurements due to satellite orbital stability.

49 Diurnal variations of temperatures themselves, in the form of thermal tides, are well known,  
50 and are a result of absorption of solar radiation (see Brasseur and Solomon [2005] and references  
51 therein).

52 Understanding the behavior of trends with local time can be important because the large  
53 majority of global temperature measurements, especially in the stratosphere, are made by sun-  
54 synchronous satellites whose instruments measure temperature at only one or two fixed local  
55 times, for the duration of their missions. In these cases, the zonal mean trends derived from  
56 various satellite data are tied to, and biased by the specific local times at which each instrument  
57 samples the data.

58 Care is then needed in comparing results of trends derived from various measurements which  
59 sample data at different local times. It is also needed when merging data from various sources to  
60 produce generic, continuous, longer-term records. In addition, the zonal means of 3D models are  
61 averages of temperatures over both longitude and the 24 hours of local time, and comparisons  
62 with trends based on data taken at fixed local times, or a subset of local times, can be  
63 problematic.

64 In the following, based on data from the Sounding of the Atmosphere using Broadband  
65 Emission Radiometry (SABER) instrument on the Thermosphere-Ionosphere-Mesosphere-  
66 Energetics and Dynamics (TIMED) satellite, we derive the local-time dependence of decadal  
67 temperature trends over the 24 hours of local time, from 2002 to 2014, from the stratosphere into  
68 the lower thermosphere (20 to 100 km), within 48° of the equator.

69 Comparable results for temperature trends have not been available previously.

70 In a previous paper, Huang and Mayr [2019] had analyzed the effects of local time on the  
71 response of temperature (and ozone) to the solar cycle (~ eleven years).

72 We find that the temperature trends, based on zonal mean measurements at a fixed local time,  
73 can be different from those based on measurements made at a different fixed local time. These  
74 variations of trends can be significant in all regions of our study, and can vary significantly even  
75 from hour to hour.

76 Our results suggest that part of the reason that temperature trends are different for different  
77 local times is that the tidal amplitudes and phases of the tides also follow trends over the time  
78 span of the data.

79 In the following, we compare with results of trends by others. Because trends vary with the  
80 time span considered, comparisons should cover similar times, and the opportunities are limited.  
81 Our results compare favorably in the stratosphere with those by Funatsu et al., [2016], based on  
82 the Advanced Microwave Sounder (AMSU) and night-time lidar measurements. In the lower  
83 thermosphere, we compare with results by She et al., [2019], also based on night-time lidar  
84 measurements. Our corresponding results agree well with the Funatsu et al., [2016] AMSU  
85 trends, but neither agrees as well with their night-time lidar results. However, our trends derived  
86 for night times agree much better with the lidar night-time results. This is also true for  
87 comparisons in the lower thermosphere with the night-time lidar results of She et al., [2019].  
88 Although the comparisons support our results of local time variations in trends, the examples do  
89 not yet a pattern make, and more comparisons are needed.

90 Global stratospheric data are largely from the NOAA series of operational satellites and the  
91 Earth Observing System of satellites. These are generally in sun-synchronous orbits, so that data  
92 are sampled at only one or two local times, which are fixed for the duration of the missions. The



93 operational satellites are meant in part to monitor the atmosphere over the longer term, and have  
94 been making measurements since the 1970s. Over the years, they are replaced as needed, in order  
95 to maintain a continuous record of data. However, there have been issues of data continuity and  
96 compatibility among the different satellites, related to data sampling, instrument calibration, and  
97 operation. Also, over the years, the orbits of some satellites have drifted from their planned sun-  
98 synchronous state, so that the local times at which the measurements are made have also drifted  
99 over several hours or more.

100 There have been group and individual efforts to combine and merge the data from different  
101 sources to obtain uniform, consistent, decades-long data bases for temperature (and others). Parts  
102 of the issues are concerned with differences due to local times when merging data. For example,  
103 Mears and Wentz [2016] have considered the sensitivity of temperature trends to “diurnal cycle  
104 adjustment”, and improved the consistencies of the different data sets caused by orbital drifts in  
105 local time, based on cross information from other satellites, and on general circulation models.  
106 Keckut et al., [2015] have also shown that considering atmospheric tides to account for  
107 differences among measurements of successive operational polar orbiting satellites would  
108 improve matters. Funatsu et al., [2008] have studied the differences among night time lidar data  
109 and daytime sun-synchronous satellite data. Randel et al, [2016], McLandress (2015), Zou et  
110 al.,[2014, 2016], among others, have also considered the issue of merged data from various  
111 sources, with consideration for differences due to effects of local time

112 These merged long-term datasets have general advantages of providing for studies of trends  
113 and responses to solar activity. However, as noted earlier, if the various data sets do not  
114 represent uniform sampling in local time, the merged data could be tagged by the biases in local  
115 times.

116

## 117 **2 Previous results**

118 Because we make use of our previous results of temperature diurnal variations and trends, we  
119 briefly review for the convenience of the reader. Our previous results on temperature trends were  
120 based only on zonal means that are averages over both longitude and local time. See Huang et  
121 al., [2014, 2010a].

122 The SABER instrument was launched in December 2001 on the TIMED satellite (Russell et  
123 al., 1999). The data used here is version 2.0, level2A. The values are interpolated to 4-degree  
124 latitude and 2.5 km altitude grids, and zonal averages are taken for analysis.

125 SABER temperature measurements have been analyzed with success by us and by others.  
126 Zhang et al. [2006] and Mukhtarov et al. [2009] have derived temperature diurnal tides using  
127 SABER data, and Nath and Sridharan [2014] have derived temperature trends using the same  
128 SABER data, but without accounting for diurnal variations. We have derived variations with  
129 periods from less than one day (diurnal variations) up to multiple years (semiannual oscillations  
130 (SAO), quasi-biennial oscillations (QBO)), and one decade or more (responses to the solar  
131 cycle). See Huang et al. [2010a, 2014, 2016a, b, 2019].

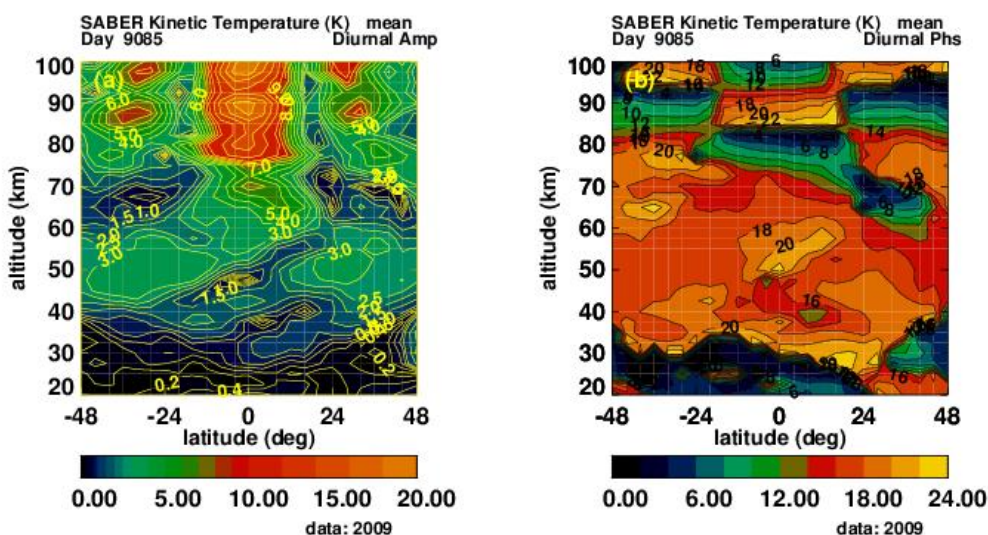
132

### 133 **2.1 Diurnal variations**

134 Due to the orbital characteristics of TIMED, SABER samples over the 24 hrs of local time and  
135 that can be used to estimate diurnal variations of temperature. As described in Huang et al.  
136 [2010a], we do this by performing a least squares fit of a two dimensional Fourier series, where  
137 the independent variables are local time and day of year.



138 Figure 1 shows an example of temperature diurnal amplitudes (left panel) and phases (right  
 139 panel) of the diurnal tide on altitude-latitude coordinates (20 to 100 km, 48°S to 48°N), for day  
 140 85 of 2009. Although not shown, higher components, such as the semidiurnal tides can also be  
 141 significant. Our derivation includes 5 Fourier components.



142  
 143 **Figure 1.** Temperature tides from 20 to 100 km, 48°S to 48°N, day 85, year 2009. Left panel (a): diurnal amplitudes  
 144 (K). Right (b): diurnal phases (hr maximum values).  
 145

146  
 147 **2.2. Mean variations.**

148 The zonal mean variations, which are averages over both longitude and local time, consistent  
 149 with 3D models, are obtained together with the diurnal variations.  
 150 Based on these zonal means, our earlier results of trends and decadal responses to solar activity  
 151 had been presented in Huang et al. [2014, 2016a, 2016b, 2019].  
 152

153 **3 Current analysis**

154 In the following, we generate

- 155 1) Monthly zonal means that are averages over longitude, but at specific local times, to
- 156 correspond to measurements by sun-synchronous satellites and night-time lidar measurements.
- 157 2) Monthly zonal means to simulate satellite orbital drifts, with local times that vary from month
- 158 to month.
- 159 3) Monthly zonal means that are averages over longitude and the 24 hours of local time, as
- 160 previously done.

161 From 1), 2), and 3) we estimate temperature trends using Equation (1), in a similar manner as  
 162 previously done by others, and by us, using a multiple regression analysis that includes solar  
 163 activity, trends, seasonal, quasi biennial oscillations (QBO), and local time terms, on monthly  
 164 values. Specifically, the estimates are found from the equation  
 165

$$166 \quad T(t) = a + b*t + c*S(t) + l*lst(t) + g*QBO(t) + d*F107(t) \quad (1)$$

167



168 where  $t$  is time (months),  $a$  is a constant,  $b$  is the trend,  $d$  the coefficient for solar activity (10.7  
 169 cm flux),  $c$  is the coefficient for the seasonal ( $S(t)$ ) variations,  $l$  the coefficient for local time ( $lst$ )  
 170 variations, and  $g$  the coefficient for the QBO. As is often done, the seasonal and local time  
 171 variations are removed first, but we include them in Equation (1) for completeness. The F107  
 172 stands for the solar 10.7 cm flux, which is commonly used as a measure of solar activity, and the  
 173 values used here are monthly means provided by NOAA.

174  $T$  stands for the various input temperature zonal means described in 1), 2), and 3), above.

175 The multiple regression is applied to the monthly zonal-mean values from June 2002 through  
 176 June 2014 from 48°S to 48°N latitude, and from 20 to 100 km.

177 The analysis of uncertainties is the same for this study as for the previous study of the mean  
 178 variations just described. Here the zonal means are generated at specific local times. Details and  
 179 results of the statistical analysis are given in Huang et al., [2014, 2106a].

180

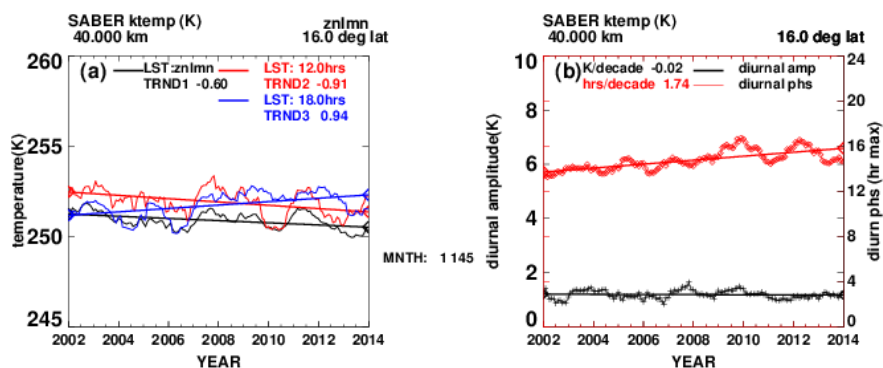
#### 181 4 Current results: temperature trends as a function of local time

182 Before presenting our overall trend results as a function of local time, we first compare some  
 183 specific results with those by others. The merged data sets noted earlier do not represent uniform  
 184 averages over the range of local times nor do they represent specific fixed local times. In  
 185 addition, they span a longer time interval than the SABER data, and we will not use them for  
 186 comparisons. Because trends can significantly depend on the particular time period, comparisons  
 187 are limited to the time span ~ 2002 to 2014.

188 Figure 2(a) (left panel) shows examples of our estimates of monthly SABER values of  
 189 temperature (K) from mid 2002 to mid 2014, without the diurnal and seasonal variations. The  
 190 black line shows zonal mean values that are averages over both longitude and local time at 40  
 191 km and 16° latitude, with a trend of ~ -0.6 K/decade, found from a linear fit. The red line shows  
 192 monthly values of zonal means at a fixed 12 hrs local time, with a trend of ~ -0.91 K/decade.  
 193 The blue line represents monthly values of zonal means at a fixed local time of 18 hrs, with a  
 194 trend of ~ +0.94 K/decade. Figure 2(b) (right panel) shows the temperature tidal diurnal  
 195 amplitude (black line, left hand scale) and the diurnal phase (red line, hour of maximum value,  
 196 right hand scale).

197 The trends of the diurnal amplitudes and phases themselves contribute to the different  
 198 temperature trends at different local times. Although not shown, we note that semidiurnal tides  
 199 are not negligible.

200



201



202 **Figure 2.** Left panel (a): Monthly SABER temperature (K) from 2002 to 2014, 40 km, 16°N latitude. Black line:  
203 zonal mean values (averages over longitude and local time); red line: zonal mean at 12 hrs local time; blue line:  
204 zonal mean at 18 hrs local time. Right panel (b): left axis scale: black line: tidal diurnal amplitude (K); red line, right  
205 axis scale: diurnal phase (hr of maximum value).  
206  
207

#### 208 **4.1 Stratosphere.**

209 For the stratosphere, we compare with trends given by Funatsu et al.,[2016], based on data  
210 from the Advanced Microwave Sounding Unit (AMSU) on the NASA Aqua satellite and from  
211 night-time ground-based lidar measurements. The results of Funatsu et al.,[2016] are suitable for  
212 comparison because the time span of the data are similar to ours (2002 to 2014), and AMSU  
213 samples data near specific local times, namely, 13:30 and 1:30 local times.

214 Following Funatsu et al.,[2016], the AMSU is a cross-scanning microwave-based sounder and the  
215 channels 9–14 sample with weighting functions peaking at approximately 18, 20, 25, 30, 35, and 40  
216 km. The horizontal resolution at the near-nadir field of view is approximately 48 km, and the vertical  
217 half width of the weighting functions is about 10 km.

218 Although the lidar measurements presented by Funatsu et al.,[2016] also cover a similar time  
219 span (2002–2013), they are made only during night time from the Observatoire de Haute  
220 Provence (OHP, 43.91°N, 5.71°E) and the Mauna Loa Observatory (MLO, 19.51°N, 155.61°W).

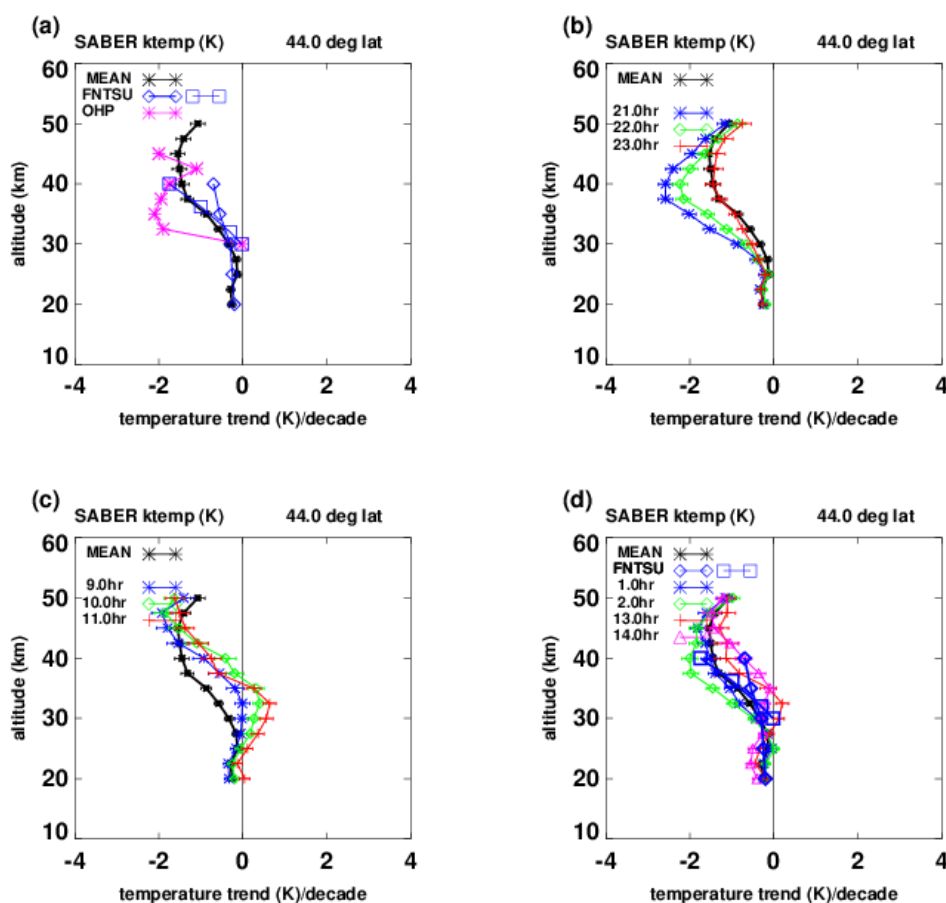
221 Figure 3 shows our results of temperature trends (K/decade) based on SABER data (2002 to  
222 2014) and those from Funatsu et al.,[2016], based on AMSU and lidar measurements. For  
223 AMSU, Funatsu et al., [2016] provide trends as a function of channel numbers for the low and mid  
224 latitude composite trends, so following McLandress et al.,[ 2015], we use the altitudes of the  
225 weighting function peaks, namely 20, 25, 30, 35, and 40 km, for comparison. They do provide  
226 altitudes in km for comparison with lidar. We note that where the values and altitudes are given by  
227 others such as Funatsu et al., [2016], we have transferred them manually to our figures, as needed.

228 In the top left panel (a) of Figure 3, the black line plots trend results based on SABER zonal  
229 means found by averages over both local time and longitude. The blue diamonds and squares are  
230 from Funatsu et al.,[2016], based on AMSU data, presumably averages taken near 1:30 and  
231 13:30 hours. The blue diamonds denote zonal mean trends for mid latitudes (30° to 60°N), and  
232 the blue squares represent trends at 44°N to correspond to OHP. The blue squares are available  
233 only from 30 to 40 km (~ 30, 32.0, 36.2, 40.0 km), but match our results (black line) at 44°N  
234 extremely well. The blue diamonds (from Funatsu AMSU, an amalgam to represent mid latitude)  
235 match our results almost exactly from 20 to 30 km, but are larger from 30 to 40km. This could  
236 simply be that the blue diamonds represent mid latitudes (30° to 60°N) while the blue squares  
237 and our black line represents trends at 44°N specifically. The magenta asterisks, also provided by  
238 Funatsu et al.,[2016], based on night-time lidar measurements at 44°N, are significantly more  
239 negative from 30 to 40 km than our results and those of the Funatsu et al.,[2016] AMSU. The top  
240 right panel (b) of Figure 3 shows our night time results from SABER at 21, 22, 23 hrs. It can be  
241 seen that our night time results agree better with the night-time lidar trends (magenta asterisks) in  
242 the left panel Figure 3(a). We do not know the details of the night-time hours of the lidar data.  
243 The bottom row left panel (c) of Figure 3 shows our daytime trends at 9, 10, 11 hrs, and agree  
244 less well with the lidar trends.

245 The average of all our night and daytime trends gives the zonal mean average shown by the  
246 black line. The bottom right panel (d) compares our results at 1, 2, 13, and 14 hrs with the  
247 AMSU results. They are near the local times of the AMSU data (presumably 1:30 and 13:30 hrs).  
248 It can be seen that the averages over the 4 local times compare favorably with those of Funatsu et



249 al., [2016], based on AMSU data. It is not clear if Funatsu et al.,[2016] differentiated night from  
250 day measurements.  
251 We believe that, by taking into account trends with local time, our results compare favorably  
252 with both the Funatsu et al., [2016] AMSU trends and their results based on night time lidar data.  
253  
254  
255



256  
257  
258 **Figure 3.** Temperature trends (K/decade, 2002-2014) vs altitude. Top left (a): Black asterisks:based on SABER  
259 zonal means (over longitude and local time) at 44°N; blue diamonds: Funitsu Aqua trends for mid latitudes (30°-  
260 60°N); blue squares: Funatsu Aqua trends at 44°N; magenta asterisks: based on night-time lidar measurements at  
261 OHP (44°N). Top right (b): Black asterisks: same as (a), blue, green, red: our estimates at 21, 22, 23 hrs local time,  
262 based on SABER data. Bottom left (c): Black asterisks: same as (a), blue, green, red: our estimates at 9, 10, 11 hrs  
263 local time; bottom right (d): Black asterisks, same as (a); blue diamonds and squares: as in panel (a), Funatsu  
264 AMSU, blue asterisks, green diamonds, red plusses, magenta triangles: SABER trends at 1, 2, 13, 14 hours.  
265

266 The left panel of Figure 4 corresponds to that of Figure 3, but for 20°N to compare with  
267 results of Funatsu et al., [2016] based on AMSU low-latitude and night-time lidar results at the



268 Hawaiian Mauna Loa Observatory (MLO, 19.51°N). As in Figure 3 for OHP, the lidar results  
 269 show a diversion to more negative trends near 30-35 km. Here, our results, as represented by  
 270 trends based on zonal means that are averages over local time also show a decrease, although not  
 271 as pronounced, near 30-35 km. As in Figure 3, both the blue diamonds and blue squares are from  
 272 Funatsu et al., [2016] based on AMSU data, but for low latitudes (0 to 30°N), and 20°N latitude,  
 273 respectively. They are smoother than our results between 25 and 40 km and do not show the  
 274 notch near 30 km that we and the lidar-based trends show. This could be due to the differences in  
 275 altitude resolution between AMSU and lidar and SABER data.

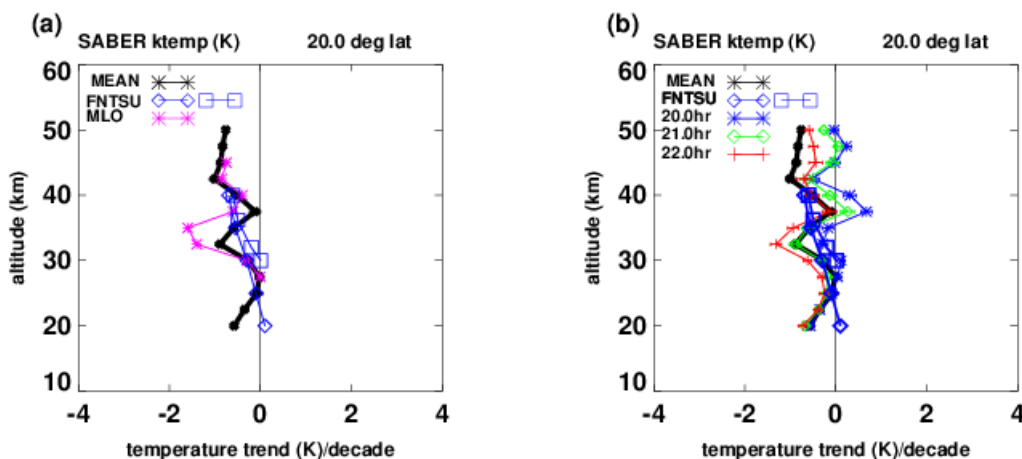
276 As can be seen in the right panel (b) of Figure 4, the decrease on our trends near 30 km is due  
 277 in large part to the behavior at 21 and 22 hours (green diamonds, red plusses).

278 Figures 3 and 4 show that by taking into account the different trends with local time, our  
 279 results compare more favorably with those of the Funatsu et al., [2016], based on AMSU and  
 280 lidar data. Figures 3 and 4 also show that trends can change significantly with local time, even  
 281 from hour to hour.

282 However, our comparisons do not a pattern make, and more comparisons are of course  
 283 needed.

284 We note that the results of Khaykin et al.,[2017] based on analysis of GPS Radio Occultation  
 285 (GRO) measurements are in excellent agreement with AMSU (based on a slightly longer period  
 286 (2002-2016). Khaykin et al.,[2017] state that, " after down sampling of GRO profiles according  
 287 to the AMSU weighting functions, the spatially and seasonally resolved trends from the two data  
 288 sets are in almost exact agreement with trends based on AMSU data."

289  
 290  
 291  
 292



293  
 294  
 295  
 296  
 297  
 298  
 299

**Figure 4.** Temperature trends (K/decade) vs altitude. Left (a): Black asterisks:trends based on SABER zonal means (over longitude and local time) at 20°N; blue diamonds: Funitsu et al.,[2016] Aqua; data at 13.5 and 1.5 hrs, low latitudes (0° to 30°N); blue squares: Funitsu Aqua at 20°N; magenta asterisks: lidar measurements at Mauna



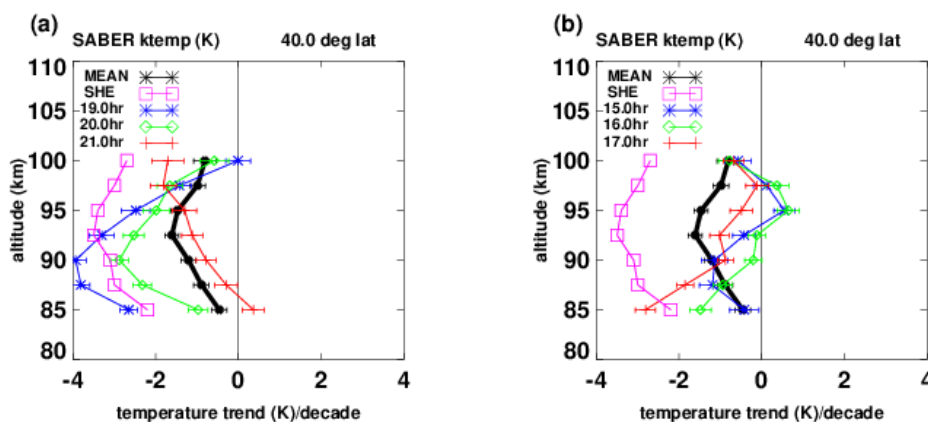
300 Loa Observatory (MLO, 19.51°N), Right (b): Black asterisks: same as (a), blue, green, red: estimates at 20, 21,  
301 22 hrs local time, based on SABER data.  
302

## 303 4.2 Lower Thermosphere

304 In Figure 5, we compare our results (K/decade) with the lidar night-time measurements of She  
305 et al.,[2019], at Fort Collins, CO. (41°N, 105°W)/Logan Utah (42°N, 112°W), from 2002-2014.  
306 They actually made nocturnal temperature observations between 1990 and 2017, but divided  
307 their analysis into various time periods, and smaller time intervals within the night time hours.  
308 This provides valuable information regarding trends and local time. In the left panel (a) of Figure  
309 5, the magenta squares denote the mean night time trends derived by She et al.,[2019]. The black  
310 line represents our trend results based on zonal means (averages over longitude and local time),  
311 while the blue asterisks, green diamonds, and red plusses show our zonal mean trends at 19, 20,  
312 and 21 hours, respectively. In contrast, the right panel (b) of Figure 5 shows corresponding  
313 results based on Saber data in the day time at 15, 16, 17 hours local time. We have not included  
314 more local times due in part that the plots become busy, and some lines reach maximum and  
315 minima at different altitudes. Overall, the averages of day time and night trends result in the  
316 black line.

317 It can be seen in Figure 5 that, as in Figures 3 and 4, changes in trends over as little as an  
318 hour of local time can be significant. These results show that there are systematic differences in  
319 derived trends at different local times. This agrees with those of She et al., [2019], who have also  
320 derived trends averaged over 2 hrs at midnight, and they are significantly different from those  
321 found from the all-night mean measurements. She et al., [2019] provide midnight results only for  
322 a much larger time span (March 1990 to December 2017), so we do not compare.

323 Considering that the lidar data are not zonal means, and the details of the night-time sampling  
324 are probably different from ours, we believe that our results generally support those of She et al.,  
325 [2019].  
326



327  
328  
329  
330  
331  
332  
333

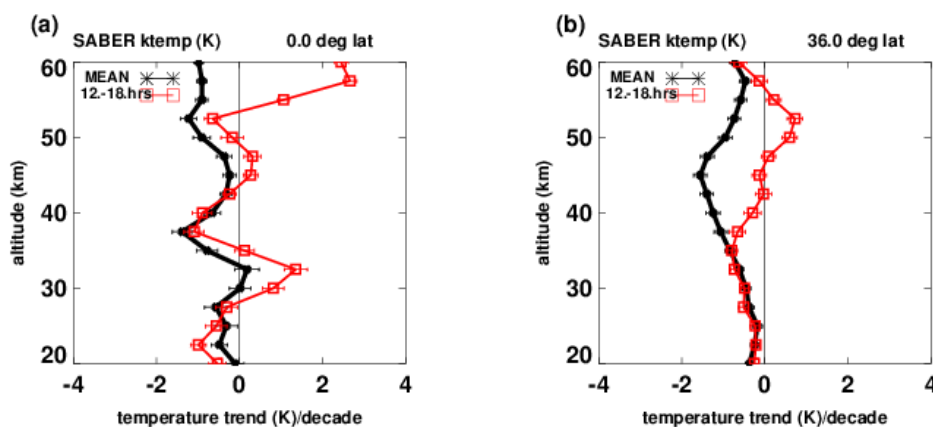
**Figure 5.** Temperature trends (K/decade) vs altitude, at 40°N latitude. Left (a): Black asterisks: trends based on SABER zonal mean (over longitude and local time); blue asterisks, green diamonds, red plusses: trends based on SABER zonal means at 19, 20, 21 hrs local time. Magenta squares: trends based on night-time lidar measurements by She et al.,[2019]; Right (b): as in (a) but for SABER results at 15, 16, 17 hrs local time.



### 334 4.3 Orbital drift and generic

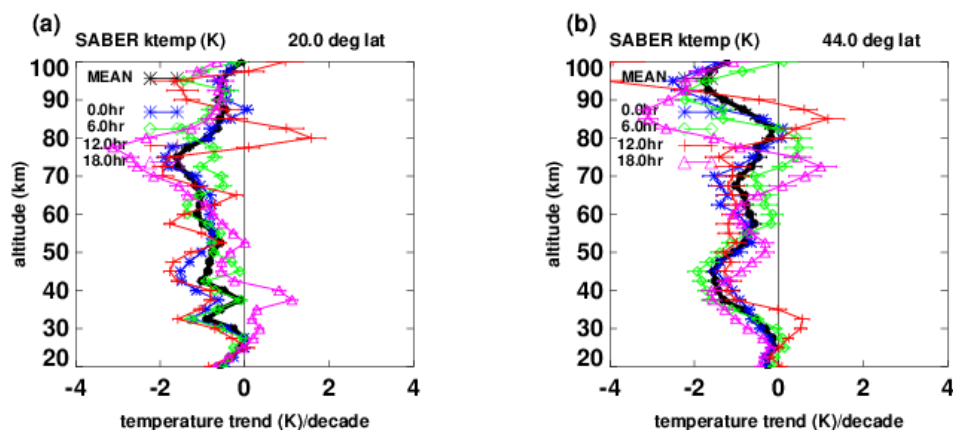
335 As noted earlier, over years, the orbits of some operational satellites have drifted from their  
336 intended sun-synchronous state, so that the local times at which measurements are made have also  
337 drifted, by several hours. We have simulated the potential changes in temperature trends. As a simple  
338 example, Figure 6 shows our results for temperature trends (K/decade) versus altitude, at the Equator  
339 (left panel) and at 36°N, from 20 to 60 km. The red squares denote trends where local times increased  
340 linearly from 12 to 18 hrs from 2002 to 2014, to simulate orbital drift. Black asterisks denote trends  
341 based on SABER data.

342 This exercise is only meant to provide order-of-magnitudes that can result when local times at  
343 which measurements are made are not controlled.  
344



345 **Figure 6.** Temperature trends (K/decade) vs altitude at the equator (left panel) and 36°N latitude (right panel).  
346 Black lines: trends based on SABER data (averaged over longitude and local time); red squares: estimated trends for  
347 cases where local times of measurements increase linearly from 12 to 18 hrs from 2002 to 2014.  
348  
349

350 Figure 7 shows more generally our derived trends (K/decade), based on SABER data, at 20°N  
351 (left panel) and 44°N (right panel), from 20 to 100 km. The blue asterisks, green diamonds, red  
352 plusses, and magenta triangles represent 0, 6, 12, and 18 hrs, respectively. A detailed analysis is  
353 beyond the scope of this study. The salient features are that the trends can vary significantly as a  
354 function of local time, even from hour to hour. These variations are also different with altitude  
355 and latitude.  
356



357  
358 **Figure 7.** Temperature trends (K/decade) vs altitude from 20 to 100 km at 20°N (left panel) and 44°N (right panel).  
359 Black: trends based on SABER zonal means over longitude and local time; blue: based on zonal means at 0 hr;  
360 green: 6 hrs, red: 12hrs, magenta: 18 hrs local time.  
361

### 362 **5 Summary and conclusion.**

363 Using SABER data, we have investigated the local time variations of temperature trends  
364 (K/decade) from 2002 to 2014, 20 to 100 km, and 48°S to 48°N latitude.

365 Our results show that the values of temperature decadal trends for a fixed local time are  
366 different from trends at another fixed local time. The temperature diurnal variations themselves  
367 are due to thermal tides. We find that the amplitudes and phases of the tides also display decadal  
368 trends and are then likely a contributor to the local time variations of temperature trends.

369 These results have not been available previously.

370 The dependence of trends on local time is significant throughout the region of analysis, and  
371 can be significant even from hour to hour, as can be seen in Figures 3, 4, 5, and 7.

372 In the lower thermosphere, this agrees with the trend results by She et al., [2019], based on  
373 lidar night-time measurements. She et al., [2019] found that trends based on a two-hour average  
374 near midnight show systematic differences from the average over other hours. Our comparisons  
375 with the overnight results of She et al., [2019] are seen in Figure 5, where our trends at 19, 20,  
376 and 21 hours compare favorably, while our day time trends at 15, 16, and 17 hours compare less  
377 favorably.

378 In the stratosphere, our comparison with trends found by Funatsu et al., [2016], based on lidar  
379 and AMSU measurements, are even better, as seen in Figures 3 and 4. At 44°N (AMSU and  
380 OHP lidar), Funatsu et al., [2016] provide AMSU trend results only from 30 to 40 km, but they  
381 match our results almost exactly. Their results from 20 to 40 km, representing mid latitudes (30°  
382 to 60°N) also match our results almost exactly from 20 to 30 km, but are larger from 30 to 40 km.  
383 Between ~ 30 to 40 km, the night-time lidar trends are significantly smaller (more negative) than  
384 both our and that of Funatsu et al., [2016]. However, when the comparison is between night time  
385 lidar and our night-time results (21, 22, and 23 hours, see Figures 3a, 3b), the agreements are  
386 better. At 20°N (AMSU and MLO lidar), similar comments apply.



387 These examples all suggest that at least some of the differences between night time lidar  
388 trends and those based on other measurements that are not made at night, can be explained at  
389 least partly, through variations of trends with local time.

390 Because our results show that the data sets representing measurements at different fixed local  
391 times can result in varying trends, merging those data can result in trends that cannot be tied to  
392 specific local times, or to averages over the 24 hours of local time, as in 3D models, and can  
393 result in biases. Although there have been previous studies related to variations with local time,  
394 they focused on mitigating differences when merging data from different sources, and on  
395 accounting for temperature variations with local time due to orbital drifts.

396 Our three examples of course do not a pattern make, and more direct comparisons are  
397 needed. Our current comparisons are limited because the various results should be based on the  
398 similar time spans, and also not based on merged data from various sources, as the identity in  
399 local time would not be clear for merged data.

400 Our results for temperature tidal amplitude and phase trends shown in Figure 2 are also  
401 derived from the same SABER data, and have not been available previously. This supports the  
402 conclusion that the dependence of temperature trends on local time is due, at least in part, to the  
403 behavior of tidal trends.

404

#### 405 **Data availability**

406 The SABER data are freely available from the SABER project at <http://saber.gats-inc.com/>.

407

#### 408 **Acknowledgements.**

409

410

#### 411 **References**

412 Brasseur, G. P. and Solomon, S.: *Aeronomy of the Middle Atmosphere*, Springer, Dordrecht,  
413 The Netherlands, 2005.

414 Funatsu, B.M., Chantal Claud, Philippe Keckhut, and Alain Hauchecorne, Cross-validation of  
415 Advanced Microwave Sounding Unit and lidar for long-term upper-stratospheric temperature  
416 monitoring, *J. Geophys Res*, 113, D23108, doi:10.1029/2008JD010743, 2008

417 Funatsu, B. M., Chantal Claud, Philippe Keckhut, Alain Hauchecorne, and Thierry Leblanc,  
418 [Regional and seasonal stratospheric temperature trends in the last decade \(2002–2014\)](#)  
419 [from AMSU observations](#), *Journal of Geophysical Research: Atmospheres*  
420 10.1002/2015JD024305, July, 2016

421 Huang, F. T., McPeters, R. D., Bhartia, P. K., Mayr, H. G., Frith, S. M., Russell III, J. M., and  
422 Mlynczak, M. G.: Temperature diurnal variations (migrating tides) in the stratosphere and lower  
423 mesosphere based on measurements from SABER on TIMED, *J. Geophys. Res.*, 115, D16121,  
424 doi:10.1029/2009JD013698, 2010a.

425 Huang, F. T., Mayr, H. G., Russell III, J. M., and Mlynczak, M. G.: Ozone and temperature  
426 decadal trends in the stratosphere, mesosphere and lower thermosphere, based on measurements  
427 from SABER on TIMED, *Ann. Geophys.*, 32, 935–949, 2014.

428 Huang, F. T., Mayr, H. G., Russell III, J. M., and Mlynczak, M. G.: Ozone and temperature  
429 decadal responses to solar variability in the mesosphere and lower thermosphere, based on  
430 measurements from SABER on TIMED, *Ann. Geophys.*, 34, 29–40, doi:10.5194/angeo-34-129-  
431 2016a.



- 432 Huang, F. T., H. G. Mayr, J. M. Russell III, and M. G. Mlynczak, Ozone and temperature  
433 decadal responses to solar variability in the stratosphere and lower mesosphere, based on  
434 measurements from SABER on TIMED, *Ann. Geophys.*, 34, 801–813, doi:10.5194/angeo-34-  
435 801-2016, 2016b.
- 436 Huang, F. T., and Hans G. Mayr, Ozone and temperature decadal solar-cycle responses, and  
437 their relation to diurnal variations in the stratosphere, mesosphere, and lower thermosphere,  
438 based on measurements from SABER on TIMED, *Ann. Geophys.*, 37, 471–485, 2019  
439 <https://doi.org/10.5194/angeo-37-471-2019>
- 440 Keckhut, P., B. M. Funatsu, C. Claudc, and A. Hauchecornea, Tidal effects on stratospheric  
441 temperature series derived from successive advanced microwave sounding units,  
442 *Quarterly Journal of the Royal Meteorological Society Q. J. R. Meteorol. Soc.* 141: 477–483,  
443 January 2015 B DOI:10.1002/qj.2368
- 444 Khaykin, S.M., B.M. Funatsu, A. Hauchecorne, S. Godin-Beekmann, C. Claud, P. Keckhut,  
445 A. Pazmino, H. Gleisner, J. K. Nielson, S. Syndergaard, and K.B. Lauritsen. [Postmillennium  
446 changes in stratospheric temperature consistently resolved by GPS radio occultation  
447 and AMSU observations](#) *Geophysical Research Letters*, 10.1002/2017GL074353, July, 2017
- 448 Mears, C. A., & Wentz, F. J. (2016). Sensitivity of satellite-derived tropospheric temperature  
449 trends to the diurnal cycle adjustment. *Journal of*  
450 *Climate*, 29, 3629–3646
- 451 McLandress, C., T. G. Shepherd, A. I. Jonsson, T. von Clarmann, and B. Funke,  
452 A method for merging nadir-sounding climate records, with an application to the global-mean  
453 stratospheric temperature data sets from SSU and AMSU, *Atmos. Chem. Phys.*, 15, 9271–9284,  
454 2015, doi:10.5194/acp-15-9271-2015
- 455 Mukhtarov, P., Pancheva, D., and Andonov, B.: Global structure and seasonal and interannual  
456 variability of the migrating diurnal tide seen in the SABER/TIMED temperatures between 20  
457 and 120 km, *J. Geophys. Res.*, 114, A02309, doi:10.1029/2008JA013759, 2009
- 458 Nath, O., and Sridharan, S.: Long-term variabilities and tendencies in zonal mean TIMED–  
459 SABER ozone and temperature in the middle atmosphere at 10–15°N, *J. Atmos. Solar-Terr.*  
460 *Phy.*, 120, 1–8, 2014.
- 461 Randel, W. J., Smith, A. K., Wu, F., Zou, C.-Z., and Qian, H.: Stratospheric temperature  
462 trends over 1979–2015 derived from combined SSU, MLS, and SABER satellite observations,  
463 *J. Climate*, 29, 4843–4859, <https://doi.org/10.1175/JCLI-D-15-0629.1>, 2016.
- 464 Russell, III J. M., Mlynczak, M. G., Gordley, L. L., Tansock, J., and Esplin, R.: An overview  
465 of the SABER experiment and preliminary calibration results, *Proceedings of the SPIE*, 44th  
466 Annual Meeting, Denver, Colorado, July 18–23, 3756, 277–288, 1999.
- 467 Zhang, X., Forbes, J. M., Hagan, M. E., Russell III, J. M., Palo, S. E., Mertens, C. J., and  
468 Mlynczak, M. G.: Monthly tidal temperatures 20–120 km from TIMED/SABER, *J. Geophys.*  
469 *Res.*, 111, A10S08, doi:10.1029/2005JA011504, 2006.
- 470 Zou, C.-Z., Qian, H., Wang, W., Wang, L., and Long, C.: Recalibration and merging of SSU  
471 observations for stratospheric temperature trend studies, *J. Geophys. Res.*, 119, 13180–13205,  
472 doi:10.1002/2014JD021603, 2014.
- 473 Zou, C.-Z., Qian, H., Stratospheric Temperature Climate Data Record from Merged SSU and  
474 AMSU-A Observations, *J. Atm. and Oceanic Tech.*, 2016, DOI: 10.1175/JTECH-D-16-0018.1  
475